

- Landscape position units (LSU) are adopted to identify priority management areas.
- A Markov chain-based surrogate model of SWAT<sup>+</sup> is proposed to identify PMAs.
- SWAT<sup>+</sup> is qualified to provide flow distribution matrix among LSUs and channels.
- LSU-based PMAs are more effective in distribution and cumulative load contributes.
- LSU-based PMAs have general applicability for various geographic environments.

1 **Abstract**

2 Priority Management Areas (PMAs) of a watershed are areas with high  
3 contributions to pollutant load of the assessment outlet such as the watershed outlet,  
4 and thus have high priorities in the decision-making of comprehensive watershed  
5 management. Existing types of spatial units used to identify PMAs are commonly based  
6 on subbasins, artificial geographic entities, and grid cells. However, these identification  
7 units cannot balance the general applicability to diverse geographic environments and  
8 the representation degree to spatial heterogeneity, which affects the effectiveness of  
9 PMAs. In this paper, we propose to adopt landscape positions along the hillslope to  
10 identify PMAs, which can be delineated by slope position units (e.g., upland, backslope,  
11 and valley). Landscape position units inherently have upstream-downstream  
12 relationships with each other and with channels. Therefore, their contributions to the  
13 assessment outlet can be quantified based on the propagation effects of hillslope routing  
14 processes and channel routing processes. The proposed method was implemented by  
15 SWAT<sup>+</sup>, the restructured and enhanced version of the Soil and Water Assessment Tool,  
16 and validated by a comparative case study at a hilly watershed in southern China by  
17 identifying PMAs of total nitrogen with landscape position units and subbasin units,  
18 respectively. The results showed that the proposed PMAs based on landscape positions  
19 have more accurate distribution and contribute 68.34% of total nitrogen on 31.76%  
20 areas of the watershed, while subbasin-based PMAs contribute less (only 56.17%) on  
21 larger (39.66%) areas. The better effectiveness of landscape position units in identifying  
22 PMAs is mainly due to their better ability to represent hillslope processes and the spatial

23 heterogeneity of underlying surface environments within subbasins.

24 **Keywords:** Priority Management Areas, Landscape positions, Spatial units,

25 Pollutant load contribution, Best Management Practices, SWAT<sup>+</sup>

# 1 **1. Introduction**

2 Priority Management Area (PMA) is a prioritizing area for management in the  
3 watershed which has a high pollutant production, and more importantly, a high  
4 contribution to the pollutant load of its direct or indirect downstream water bodies  
5 (Pionke et al., 2000; Chen et al., 2014). In the decision-making of comprehensive  
6 watershed management, PMAs are ideal spatial locations for implementing suitable  
7 Best Management Practices (BMPs) to effectively control ecological and  
8 environmental problems such as soil erosion and non-point source pollution (Shen et  
9 al., 2015; Tian et al., 2020; Guo et al., 2022). The spatial distribution of PMAs  
10 considerably impacts locations, areas, and effectiveness of configured BMPs and thus  
11 affects the cost-effectiveness of the BMP scenario (i.e., spatial configuration of multiple  
12 BMPs in the watershed) (Chiang et al., 2014; Qin et al., 2018; Wang et al., 2016; Zhu  
13 et al., 2021). Therefore, accurately identifying PMAs becomes a key issue for  
14 comprehensive watershed management (Chen et al., 2022).

15 The foremost step of identifying PMAs is to determine an appropriate type of  
16 spatial units as computing units for pollutant production and contribution to the  
17 assessment outlet such as the watershed outlet (hereafter referred to as identification  
18 units) (Dong et al., 2018; White et al., 2009). Identification units adopted in existing  
19 research are mainly based on three concepts, including subbasins (Shang et al., 2012;  
20 Chen et al., 2014; Shen et al., 2015; Dong et al., 2018), artificial geographic entities  
21 (Tian et al., 2020), and grid cells (Kovacs et al., 2012).

22 Subbasin represents a relatively closed and independent geographic unit that is  
23 linked to other subbasins through channels. Subbasin units are the most straightforward  
24 and frequently used identification units since they are delineated in most watershed  
25 modeling. In addition to directly utilizing subbasin units, researchers also use the  
26 combination of subbasins as identification units according to administrative regions  
27 (such as villages; Shang et al., 2012), for the benefit of making and implementing  
28 watershed management policies (Liu et al., 2019; Shang et al., 2012). However, a  
29 subbasin can be recognized and modeled as an integral of one or more levels of finer  
30 spatial units in order to better represent spatial heterogeneity within it, such as hillslopes,  
31 slope position units, landuse fields, and even grid cells. Therefore, it may be too coarse  
32 to use these subbasin-based identification units since the heterogeneity of pollutant  
33 sources and transportation processes within subbasins should be concerned (Qin et al.,  
34 2018; Wang et al., 2016).

35 Artificial geographic entities refer to artificial constructed and hydrologically  
36 connected geographic entities according to characteristics of a specific geographic  
37 environment (Ghebremichael et al., 2013), such as polders that developed in lowland  
38 plains with densely distributed rivers and lakes (Tian et al., 2020). Such spatial units  
39 have relative homogenous features in perspectives of physical geographic processes  
40 and/or anthropogenic activities. For example, a polder may contain agricultural land,  
41 irrigation channels, ponds, and even villages, that are enclosed by artificial dams to  
42 perform as a conservation area for flood and waterlogging. Although artificial  
43 geographic entities are quite appropriate to be used as identification units in

44 corresponding geographic environments, they are not easy to be generalized as  
45 generally applicable identification units and applied widely.

46 Grid cells are commonly used spatial units with regular shapes in geographic  
47 modeling, whose underlying surface characteristics are considered to be homogeneous.  
48 Using watershed models that explicitly represent flow routings among grid cells, PMAs  
49 can be accurately identified (Kovacs et al., 2012). However, using grid cells may cause  
50 more fragmented distributions of PMAs, which reduces the implementation  
51 efficiency and limits further applications (e.g., the PMA-based spatial optimization of  
52 BMPs).

53 Therefore, existing spatial units used for identifying PMAs still cannot balance the  
54 general applicability to diverse geographic environments and the representation degree  
55 to spatial heterogeneity. According to the previous analysis, proper identification units  
56 should: 1) not be related to a specific geographic environment, 2) be capable to  
57 represent the spatial heterogeneity of underlying surface characteristics, physical  
58 geographic processes, and/or anthropogenic activities inside the study area by a small  
59 number of units, and 3) have hydrologic connections among each other.

60 In this study, we propose to use landscape positions along hillslopes within each  
61 subbasin to identify PMAs. Landscape positions can be delineated by landform units  
62 (also refers to slope position units) that reflect the integrated effects of hillslope  
63 processes on topography and affect geographic processes on the surface meanwhile  
64 (Volk et al., 2007; Arnold et al., 2010; Miller and Schaetzl, 2015; Qin et al., 2018).  
65 Landscape position units are universality for most geographic environments (Wolock

66 et al., 2004). Based on commonly used classification systems of slope positions (e.g.,  
67 the divide, backslope, and valley units adopted by Arnold et al. (2010)), each subbasin  
68 only needs a few spatial units (e.g., three in Arnold et al. (2010)) to represent the spatial  
69 homogenous from the perspective of hillslope processes (Qin et al., 2018; Rathjens et  
70 al., 2016). Besides, landscape position units have inherent upstream-downstream  
71 relationships among each other, which have been considered in watershed modeling  
72 (Arnold et al., 2010; Bieger et al., 2019; Rathjens et al., 2015; Yang et al., 2002) and  
73 spatial optimization of BMPs (Qin et al., 2018; Zhu et al., 2019; Zhu et al., 2021). Thus,  
74 landscape position units meet the requirements to be used as identification units  
75 mentioned above.

76 The remaining sections of this paper are organized as follows. Section 2 introduces  
77 the proposed method of identifying PMAs based on landscape positions. Section 3  
78 presents a comparative experimental design of using landscape position units and  
79 subbasin units respectively to identify PMAs of total nitrogen in a small hilly watershed  
80 of Southern China based on the same SWAT<sup>+</sup> model, i.e., the restructured and enhanced  
81 version of the SWAT (Soil and Water Assessment Tool). Experimental results and  
82 discussion are given in Section 4, and conclusions in Section 5.

## 83 **2. Method design**

84 To identify PMAs at the landscape position unit level, two key issues should be  
85 addressed. The first is how to quantify pollutants released at landscape position units.  
86 The second is how to distinguish the pollutant load contribution of each landscape

87 position unit to the assessment outlet, i.e., the residual amount of pollutant after  
88 transporting to its direct downstream channel and then transitioning in hierarchical  
89 channels before reaching the assessment outlet (Chen et al., 2014).

90 Generally, the pollutant load contribution cannot be directly found in the result of  
91 most watershed models. Instead, watershed models output the pollutant released from  
92 each simulation unit (e.g., HRU (Hydrologic Response Unit) in SWAT) or lumped unit  
93 (e.g., subbasin), as well as the flow in and out of substances of each channel. To fill this  
94 gap, Grimvall and Stålnacke (1996) proposed a Markov chain-based surrogate model  
95 to simulate pollutant transitions from upstream channels (subbasins) to the assessment  
96 outlet in a statistical way. Their basic idea is to analog pollutant transformation and  
97 transfer processes in hierarchical channels as the Markov process, where the transition  
98 matrix is determined by upstream-downstream relationships among channels and  
99 retention effects of the channel routing process. After a finite number of transitions  
100 (equal to the length of the longest branch in hierarchical channels), all pollutants from  
101 upstream subbasins reach the assessment outlet, and corresponding pollutant load  
102 contributions can thus be derived (Grimvall and Stålnacke, 1996).

103 Follow-up studies continued to consider the subbasin as a whole in the Markov  
104 chain-based model (Chen et al., 2014; Rankinen et al., 2016), including pollutant  
105 production at hillslopes and pollutant routing in the channel. If we can separate these  
106 two processes at landscape position units and in channels, respectively, the Markov  
107 chain-based model will be able to distinguish the pollutant contribution of each  
108 landscape position unit to the assessment outlet. Based on this basic idea, the proposed

109 method aims at incorporating a watershed model that supports landscape position units  
110 as simulation units or lumped units to improve the Markov chain-based PMA  
111 identification method from the subbasin level to the landscape position unit level.  
112 Therefore, the Markov chain-based PMA identification method can be generalized as a  
113 method framework that supports hierarchical spatial units with explicit hydrological  
114 connection (i.e., upstream-downstream relationships) such as subbasins and landscape  
115 position units (Fig. 1).

## 116 **2.1 Delineation and modeling of landscape position units in SWAT<sup>+</sup>**

117 As a restructured and enhanced version of the SWAT model, SWAT<sup>+</sup> (Bieger et al.,  
118 2017, 2019) introduced a new type of spatial unit between subbasin unit and HRU  
119 named landscape position unit (LSU), the default including upland and floodplain (Fig.  
120 2). That means the basic spatial discretization of a watershed in SWAT<sup>+</sup> contains three  
121 types of nested spatial units as a hierarchy, i.e., subbasin, LSU, and HRU. Besides,  
122 SWAT<sup>+</sup> also abstracts specific types of geographic entities as spatial units with locations  
123 and properties to participate in watershed modeling. For example, reservoirs or ponds  
124 within a subbasin are firstly generalized as a whole as one point in the channel which  
125 divides the channel into two parts, and then defined by the upstream part with additional  
126 properties such as storage capacity (Fig. 2). Hillslopes, LSUs, and HRUs will also be  
127 delineated accordingly, while two aquifer units remain unchanged (Fig. 2). These  
128 spatial units can enrich the flow routing network of SWAT<sup>+</sup> and play important roles in  
129 the simulation of study areas with specific geographic environments, e.g., agricultural  
130 ecosystems with densely distributed ponds.

131 With the new spatial discretization scheme, SWAT<sup>+</sup> improved the representation  
132 of realistic hydrologic processes from hillslope to channel (Bieger et al., 2019). Instead  
133 of directly adding all released substances of HRUs (including water, sediment,  
134 pollutants, etc.) to the channel, SWAT<sup>+</sup> firstly lumps HRUs' outputs at the LSU level  
135 and then routes to other spatial units in two different methods. For surface runoff, the  
136 water from upland is distributed downstream into two portions, one directly added to  
137 the channel/pond/reservoir (e.g., 0.30 from LSU2 to the pond and 0.66 from LSU4 to  
138 the channel as shown in Fig. 2, hereafter referred to as channel collectively) and the  
139 other portion to floodplain as additional net precipitation to participate in the simulation,  
140 while the output from floodplain drains into the channel entirely (Fig. 2). The above-  
141 mentioned flow distribution ratio of surface runoff from upland is set by the area ratio  
142 of upland and hillslope by default and can be calibrated. The other method of flow  
143 routing from LSU to other spatial units is completely draining from upland to floodplain  
144 and from floodplain to channel, which is applicable for lateral flow in soils and  
145 groundwater recharge in aquifers (Fig. 2).

146 Therefore, with the flow routing network primarily constructed by HRU, LSU,  
147 and channel (Fig. 2), SWAT<sup>+</sup> is qualified to quantify pollutants released at landscape  
148 position units and corresponding transportation amounts to their direct channel.

## 149 **2.2 Pollutant load contribution of landscape position units derived** 150 **from a Markov chain-based surrogate model of SWAT<sup>+</sup>**

151 Based on the flow routing network and simulation results of SWAT<sup>+</sup>, the key part  
152 of the Markov chain-based surrogate model can be determined, that is the transition

153 matrix of pollutants through LSUs and channels. Then, with the lumped simulation  
 154 results at LSUs as inputs, the Markov chain-based model can figure out the pollutant  
 155 load contribution of each landscape position unit.

156 **2.2.1 Transition matrix of pollutants based on flow routing network and retention**  
 157 **effects of channel routing process**

158 The transition matrix is constructed by flow distribution relationships from  
 159 upstream units to downstream units and retention coefficients of channel routing  
 160 processes (Chen et al., 2014). According to the spatial discretization scheme of SWAT+  
 161 (see section 2.1), flow distribution relationships among LSUs and channels can be  
 162 represented by an  $n \times n$  matrix  $H$  (Eq. 1). Fig. 3 gives an example of the matrix  $H$ .

$$163 \quad H(i, j) = \begin{cases} s, & \text{if LSU (floodplain) } j \text{ is adjacent downstream of LSU (upland) } i \\ 1-s, & \text{if CHA } j \text{ is direct downstream of LSU (upland) } i \\ 1, & \text{if CHA } j \text{ is adjacent downstream of CHA } i \text{ or LSU (upland) } i \\ 0, & \text{otherwise} \end{cases} \quad (1)$$

164 where  $n$  is the total number of LSUs and channels in the watershed and  $s$  is the flow  
 165 distribution ratio from upland to floodplain, for surface runoff,  $s$  is initially set by the  
 166 area ratio of upland and hillslope, while for lateral flow and groundwater recharge,  $s$   
 167 equals 1 (Fig. 2). Each row represents flow distribution relationships of one spatial unit  
 168 with its downstream units. The sum of all elements in one row equals 1 except the  
 169 channel row where the assessment outlet is located (e.g., the 7<sup>th</sup> row in Fig. 3 when the  
 170 outlet of channel 7 is the assessment outlet). To a given assessment outlet of channel  $k$ ,  
 171 there exists a smallest integer  $N_k$  to make  $H^{N_k} = 0$ , that means after  $N_k$  times of  
 172 transitions, pollutants from all upstream spatial units of channel  $k$  will reach the outlet.

173 The physical meaning of  $N_k$  is the longest routing length from uppermost spatial units  
 174 to the outlet of channel  $k$ , e.g.,  $N_7$  equals 4 in Fig. 3.

175 The complicated channel routing process accounting for pollutant transformation  
 176 and transfer processes can be simplified by a retention coefficient (i.e., removal  
 177 capacity of pollutants) to be used as a surrogate calculation method (Chen et al., 2014;  
 178 Grimvall and Stålnacke, 1996; Hejzlar et al., 2009). The landscape position unit is a  
 179 lumped unit of pollutant sources calculated at HRUs and thus has no retention effect.  
 180 The retention coefficient  $R$  is also represented by an  $n \times n$  matrix as follows:

$$181 \quad R = \begin{pmatrix} r_1 & 0 & \cdots & 0 \\ 0 & r_2 & \cdots & 0 \\ \vdots & \vdots & \ddots & \vdots \\ 0 & 0 & \cdots & r_n \end{pmatrix} \quad (2)$$

182 where the  $i$ th diagonal element  $r_i$  denotes the retention coefficient of spatial unit  $i$ , for  
 183 LSUs,  $r_i$  equals to 0, for channels,  $r_i$  can be calculated by simulation results of channels:

$$184 \quad r_j = (\text{Load}_{\text{in}} - \text{Load}_{\text{out}}) / \text{Load}_{\text{in}} \quad (3)$$

185 where  $\text{Load}_{\text{in}}$  is the pollutant input to the channel  $j$  that including pollutant outputs of  
 186 adjacent upstream channels and pollutant released from upstream LSUs;  $\text{Load}_{\text{out}}$  is the  
 187 pollutant output at the outlet of the channel  $j$ .

188 The transition matrix  $\tilde{H}$  of the Markov chain-based model can be represented as  
 189 follows and thus be used to simulate flow transitions of substances (e.g., water and  
 190 pollutant) through the hierarchy of landscape position units and channels:

$$191 \quad \tilde{H} = H (I - R) \quad (4)$$

192 where  $I$  is an identity matrix.

193 **2.2.2 Calculation of pollutant load contribution**

194 Except for the transition matrix, pollutant released from each LSU are primary  
 195 input data for the Markov chain-based model as initial states. Since the channel acts as  
 196 a receptor of pollutants, it has no self-generated pollutants. An  $n \times 1$  matrix  $L$  is used  
 197 to organize the input of pollutant sources:

$$198 \quad L = (e_1, e_2, \dots, e_i, \dots, e_n)^T \quad (5)$$

199 where  $e_i$  is the pollutant released from the spatial units  $i$  based on the simulation results  
 200 of SWAT<sup>+</sup>. Specifically,  $e_i$  is equal to 0 if  $i$  is a channel.

201 The pollutant load contribution of each spatial unit to a specific assessment outlet  
 202 can be calculated by simple matrix calculations (Grimvall and Stålnacke, 1996):

$$203 \quad E = (\tilde{H}_k)^{N_k} V_k * L \quad (6)$$

$$204 \quad \tilde{H}_k(i, j) = \begin{cases} \tilde{H}(i, j), & \text{if } i \neq k \\ 1, & \text{if } i = j = k \\ 0, & \text{if } i = k \text{ and } j \neq k \end{cases} \quad (7)$$

$$205 \quad V_k(i) = \begin{cases} 1, & \text{if } i = k \\ 0, & \text{otherwise} \end{cases} \quad (8)$$

206 where  $k$  represents the assessment outlet located channel and the corresponding  
 207 modification from  $\tilde{H}$  to  $\tilde{H}_k$  implies the  $k$ th state is transformed to an absorbing state.  
 208  $V_k$  is an  $n \times 1$  matrix for extracting the  $k$ th column of  $(\tilde{H}_k)^{N_k}$ , resulting the contribution  
 209 rate of each unit. The \* denotes element-wise multiplication.

210 Considering the interested pollutant may have various states that modeled in  
 211 different watershed processes, the calculation of pollutant load contribution should be  
 212 combined by all components calculated by different transition matrix and pollutant

213 source matrix. For example, the total nitrogen considered in this study mainly includes  
 214 the nitrate nitrogen ( $NO_3$ ) and the organic nitrogen ( $ORGN$ ). Therefore, the total  
 215 nitrogen load contribution can be calculated as follows:

$$216 \quad E_{TN} = E_{NO_3-SURF} + E_{NO_3-LAT} + E_{NO_3-GW} + E_{ORGN} \quad (9)$$

$$217 \quad E_{NO_3-SURF} = (H_{SURF} (I - R_{NO_3})_k)^{N_k} V_k * L_{NO_3-SURF} \quad (10)$$

$$218 \quad E_{NO_3-LAT} = (H_{LAT} (I - R_{NO_3})_k)^{N_k} V_k * L_{NO_3-LAT} \quad (11)$$

$$219 \quad E_{NO_3-GW} = (H_{GW} (I - R_{NO_3})_k)^{N_k} V_k * L_{NO_3-GW} \quad (12)$$

$$220 \quad E_{ORGN} = (H_{SURF} (I - R_{ORGN})_k)^{N_k} V_k * L_{ORGN-SURF} \quad (13)$$

221 where  $SURF$  denotes surface runoff,  $LAT$  denotes lateral flow,  $GW$  denotes groundwater  
 222 recharge.  $H_{SURF}$ ,  $H_{LAT}$ , and  $H_{GW}$  describe the flow distribution relationships among  
 223 spatial units on surface runoff, lateral flow, and groundwater recharge, respectively.  
 224  $L_{NO_3-SURF}$ ,  $L_{NO_3-LAT}$ , and  $L_{NO_3-GW}$  are the amount of  $NO_3$  released in surface runoff, lateral  
 225 flow, and groundwater recharge, respectively;  $L_{ORGN-SURF}$  is the amount of  $ORGN$   
 226 released in surface runoff.

### 227 **2.2.3 PMA identification based on classification of pollution degrees**

228 Once the pollutant load contribution of each landscape position unit is  
 229 distinguished, a classification of pollution degrees can be adopted to identify different  
 230 levels of PMAs such as high-, medium-, and low-contribution PMAs. The classification  
 231 methods in existing studies include the standard deviation method, the Natural Breaks  
 232 method, and the water quality control targets method (Chen et al., 2014; Giri et al.,  
 233 2016), etc.

## 234 **3. Experimental design**

235 To illustrate the effectiveness of the proposed method, a comparative experimental  
236 study was design to identify PMAs of total nitrogen at landscape position level and  
237 subbasin level based on the same calibrated SWAT<sup>+</sup> model.

### 238 **3.1 Study area and data**

239 The Zhongtianshe watershed (~42 km<sup>2</sup>), located in the south of Liyang City,  
240 Jiangsu Province, China (Fig. 4), is a typical hilly area situated at the upstream region  
241 of Lake Tai. The study area is represented as a subtropical monsoon climate. The  
242 average annual temperature is 15.5°C. The average annual precipitation is 1160 mm.  
243 The main soil type is yellow-red soil, a type of acidic soil that easy to be weathered.  
244 The main land use types are forest (77%), cropland (10%, primarily paddy field),  
245 orchard (3%), residential area (8%), and water area (2%). The watershed has frequent  
246 agriculture activities, and the cultivation of rice and wheat is the primary contribution  
247 to local non-point source pollution. Since the study area is on the drinking water source  
248 of Liyang, knowing the details of the pollution situation and take reasonable measures  
249 to control it becomes a vital issue for the local government (Shi et al., 2021).

250 The data of the study area for SWAT<sup>+</sup> modeling consists of Digital Elevation  
251 Model (DEM), land use types, soil types and properties, meteorological data,  
252 agricultural management practices and the observed flow and total nitrogen data at the  
253 watershed outlet. The detailed data description is shown in Table 1.

254

### 255 **3.2 Modeling and calibration of the SWAT<sup>+</sup> model**

256 A SWAT<sup>+</sup> model (version 59.3) was built to simulate the total nitrogen pollution in  
257 the study area. Since there are more than a hundred small ponds scattered in the study  
258 area, taking the representation of ponds into consideration in the model is very  
259 necessary. Based on the location and area of real ponds, six ponds were generalized in  
260 the watershed as shown in Fig. 4. Finally, a total of 15 subbasins, 41 LSUs, and 1260  
261 HRUs were generated (Fig. 5).

262 Limited by the available observed data, we set the year of 2011 as a warm-up  
263 period, 2012–2013 and 2014–2015 as calibration and validation periods for flow  
264 modeling at the daily time step, respectively. The model performance of the total  
265 nitrogen was only calibrated by the 5-day monitoring data from 2014 to 2015 without  
266 validation.

267 The model performance was evaluated by Nash-Sutcliffe efficiency (NSE, Nash  
268 and Sutcliffe, 1970), percentage bias (PBIAS), root mean square error-standard  
269 deviation ratio (RSR), and  $R^2$ , as shown in Fig. 6 and Fig 7. The calibration of flow had  
270 an NSE, PBIAS, RSR, and  $R^2$  of 0.48, 13.36%, 0.72, and 0.52, respectively. At the  
271 period of validation, the NSE, PBIAS, RSR, and  $R^2$  were 0.52, 12.55%, 0.69, and 0.59,  
272 respectively. According to the criteria of monthly model performance proposed by  
273 Moriasi et al. (2007), the calibrated SWAT<sup>+</sup> model has an approximately satisfactory  
274 performance for flow modeling of the study area. For total nitrogen, the NSE, PBIAS,  
275 RSR, and  $R^2$  of the calibration period were 0.27, -16.57%, 0.86, and 0.40, respectively.  
276 Considering a shorter time step may cause poorer model performance (Engel et al.

277 2007), and the simulation trend was quite consistent with the observed data ( $R^2=0.40$ ),  
278 we believe the calibrated model is applicable for the validation of the proposed PMA  
279 identification method in this study.

### 280 **3.3 Identification and evaluation of PMAs at LSU level and subbasin** 281 **level**

282 To evaluate the effectiveness of PMAs at the LSU level, we also identified PMAs  
283 at the subbasin level in the same study area based on the same calibrated SWAT<sup>+</sup> model.

284 The average annual total nitrogen of the calibration period (2014–2015) was used  
285 to calculate the TN load contribution with the watershed outlet set as the assessment  
286 outlet. The standard deviation classification method was adopted to classify the TN load  
287 contribution of spatial units into three classes (Table 2). In this study, high-contribution  
288 areas were identified as PMAs.

289 The comparison of PMAs identified at the LSU level and subbasin level is  
290 conducted from two perspectives, i.e., the spatial distribution and cumulative load  
291 contributions. The spatial distribution of PMAs is an intuitive way to qualitatively  
292 analyze the spatial consistency and difference from different units. The cumulative load  
293 contributions are used to quantitatively compare the relationships between areas of PMAs  
294 and their total pollutant load contribution.

## 295 **4. Experimental results and discussion**

### 296 **4.1 Spatial distribution of PMAs**

297 Fig. 8 shows the ranking (labeled number in descending order) and classification  
298 of total nitrogen contribution at the LSU level and subbasin level, respectively. A total  
299 of 9 LSUs and 3 subbasins that classified as high-contribution areas are identified as  
300 PMAs.

301 Firstly, the classification maps of load contribution at both levels show a consistent  
302 spatial pattern. For example, low-contribution areas are almost identical, and the 2nd  
303 ranked subbasin (#2 in Fig. 8b) and its two LSUs (#2 and #3 in Fig. 8a) are all identified  
304 as PMAs.

305 Secondly, PMAs identified at the LSU level have a more accurate distribution and  
306 thus can represent the heterogeneity within subbasins to a certain extent. For example,  
307 two uplands (#12 and #15 in Fig. 8a) in high-contribution subbasins (#1 and #3 in Fig.  
308 8b) are identified as medium-contribution LSU, while some floodplains (#6 and #7 in  
309 Fig. 8a) in medium-contribution subbasins (#5 and #8 in Fig. 8b) are identified as high-  
310 contribution LSU. Besides, comparing Fig. 8a with Fig. 4b, a relatively higher  
311 correlation of LSU-based PMAs with the distribution of the cropland (i.e., the main  
312 source of the local non-point source pollution) can be found, which is more reasonable.

313 Lastly, PMAs identified based on LSUs include not only floodplain located on the  
314 bottom of hillslopes and near channel but also uplands. With the consideration of  
315 generalized ponds in SWAT<sup>+</sup>, one part of hillslope (floodplain #10 and upland #12 in

316 Fig. 8a) in the high-contribution subbasin #1 is excluded in high-contribution LSUs.  
317 These all proved that SWAT<sup>+</sup> is well qualified to characterize pollutants released at the  
318 LSU level and its transitions in the reconstructed routing network by LSUs and channels  
319 (including ponds). Therefore, the proposed PMA identification method at landscape  
320 position units using SWAT<sup>+</sup> is effective.

## 321 **4.2 Cumulative load contribution**

322 To quantitatively evaluate the difference of PMAs identified at the LSU level and  
323 subbasin level, each type of spatial unit is ranked by load contribution in descending  
324 order and plotted in Fig. 9 with the cumulative area and load contribution calculated.  
325 As shown in Fig. 9a, LSU-based PMAs contribute 68.34% of total nitrogen on 31.76%  
326 of the watershed area, while subbasin-based PMAs only contribute 56.17% on as much  
327 as 39.66% areas. That means landscape position units are more effective to identify  
328 PMAs. Besides, it is clear that the cumulative area-contribution line of the LSU-based  
329 method in Fig. 9a is always higher than that of the subbasin-based method, proving the  
330 better effectiveness although based on different types of identification units.

331 From Fig. 9 we can recognize that there is no deterministic relationship between  
332 the area of the spatial unit and its pollutant load contribution. For example, LSU #1  
333 contributes 11.97% of total nitrogen but ranks 17 in area, while subbasin #1 contributes  
334 24.27% of total nitrogen with the 2<sup>nd</sup> largest area (12.03% of the watershed). The curves  
335 in Fig. 9b and Fig. 9c indicate that the cumulative load contribution curve and  
336 cumulative area curve at the subbasin level have a more consistent variation trend than  
337 the LSU level. The comparison shows that the load contribution at the subbasin level is

338 more dependent on the area. This is because the pollutant source of nitrogen is highly  
339 related to cropland in this study area and the identification of subbasin-based PMAs is  
340 ensured by the larger area, which in turn also illustrates that landscape position units  
341 have better representations of spatial heterogeneity of landuse than subbasins.

342 From both perspectives of the spatial distribution and the cumulative load  
343 contribution, identifying PMAs at the landscape positions performs better than  
344 subbasins. LSU-based PMAs have the merit of accounting for more pollutant load  
345 contribution with smaller areas and thus can be effectively utilized in the spatial  
346 configuration of BMPs for the watershed integrated management.

## 347 **5. Conclusions**

348 This paper proposes to use landscape position units (LSUs), derived from a  
349 universal type of spatial unit for most geographic environments, as identification units  
350 for priority management areas (PMAs). A Markov chain-based surrogate model of the  
351 SWAT<sup>+</sup> model is proposed to distinguish the pollutant load contribution of each LSU to  
352 the assessment outlet and then identify PMAs according to a classification method.  
353 Experimental results show that landscape position units perform better effectiveness  
354 than widely used subbasins in identifying PMAs for their better ability to represent  
355 hillslope processes and the spatial heterogeneity of underlying surface environments  
356 within subbasins. Therefore, LSU-based PMAs are much more valuable in providing  
357 accurate locations to implement suitable best management practices for integrated  
358 watershed management.

359 The improved Markov chain-based PMA identification method can be regarded as  
360 a method framework. More types of spatial units with explicit upstream-downstream  
361 relationships may be proposed and validated for identifying PMAs with the support of  
362 proper watershed models. Besides, several issues may be worth attention in future  
363 research, for example, 1) how to consider various climate scenarios in determining  
364 retention effects of channel routing processes; 2) how a specific type of identification  
365 unit take effects on the identification of PMAs under different delineation methods; 3)  
366 how PMAs derived from different identification units affect the effectiveness and  
367 efficiency of spatial optimization of BMPs.

## 368 **Acknowledgement**

369 Supports to A-Xing Zhu through the Vilas Associate Award, the Hammel Faculty  
370 Fellow Award, and the Manasse Chair Professorship from the University of Wisconsin-  
371 Madison are greatly appreciated.

## 372 **Funding**

373 The work reported here was supported by grants from National Natural Science  
374 Foundation of China (Project No.: 41871362, 42101480, 41871300) and the 111  
375 Program of China (Approved Number: D19002).

## 376 **References**

377 Arnold, J., Allen, P., Volk, M., Williams, J.R., Bosch, D., 2010. Assessment of different representations  
378 of spatial variability on SWAT model performance. *Transactions of the ASABE*. 53(5), 1433–1443.  
379 <https://doi.org/10.13031/2013.34913>.

380 Bieger, K., Arnold, J.G., Rathjens, H., White, M.J., Bosch, D.D., Allen, P.M., 2019. Representing the  
381 connectivity of upland areas to floodplains and streams in SWAT+. *J. Am. Water Resour. Assoc.*  
382 55(3), 578–590. <https://doi.org/10.1111/1752-1688.12728>.

383 Bieger, K., Arnold, J.G., Rathjens, H., White, M.J., Bosch, D.D., Allen, P.M., Volk, M., Srinivasan, R.,  
384 2017. Introduction to SWAT+, a completely restructured version of the Soil and Water Assessment  
385 Tool. *J. Am. Water Resour. Assoc.* 53(1), 115–130. <https://doi.org/10.1111/1752-1688.12482>.

386 Chen, L., Li, J., Xu, J., Liu, G., Wang, W., Jiang, J., Shen, Z., 2022. New framework for nonpoint source  
387 pollution management based on downscaling priority management areas. *J. Hydrol.* 606, 127433.  
388 <https://doi.org/10.1016/j.jhydrol.2022.127433>.

389 Chen, L., Zhong, Y., Wei, G., Cai, Y., Shen, Z., 2014. Development of an integrated modeling approach  
390 for identifying multilevel non-point-source priority management areas at the watershed scale. *Water*  
391 *Resour. Res.* 50(5), 4095–4109. <https://doi.org/10.1002/2013WR015041>.

392 Chiang, L.C., Chaubey, I., Maringanti, C., Huang, T., 2014. Comparing the selection and placement of  
393 best management practices in improving water quality using a multiobjective optimization and  
394 targeting method. *Int. J. Environ. Res. Public Health* 11(3), 2992–3014.  
395 <https://doi.org/10.3390/ijerph110302992>.

396 Dong, F., Liu, Y., Wu, Z., Chen, Y., Guo, H., 2018. Identification of watershed priority management areas  
397 under water quality constraints: A simulation-optimization approach with ideal load reduction. *J.*  
398 *Hydrol.* 562, 577–588. <https://doi.org/10.1016/j.jhydrol.2018.05.033>.

399 Engel, B., Storm, D., White, M., Arnold, J., Arabi, M., 2007. A hydrologic/water quality model  
400 application protocol. *J. Am. Water Resour. Assoc.* 43(5), 1223–1236. [https://doi.org/10.1111/j.1752-](https://doi.org/10.1111/j.1752-1688.2007.00105.x)  
401 [1688.2007.00105.x](https://doi.org/10.1111/j.1752-1688.2007.00105.x).

402 Ghebremichael, L.T., Veith, T.L., Hamlett, J.M., 2013. Integrated watershed- and farm-scale modeling  
403 framework for targeting critical source areas while maintaining farm economic viability. *J. Environ.*  
404 *Manage.* 114, 381–394. <https://doi.org/10.1016/j.jenvman.2012.10.034>.

405 Giri, S., Qiu, Z., Prato, T., Luo, B., 2016. An integrated approach for targeting critical source areas to  
406 control nonpoint source pollution in watersheds. *Water Resour. Manage.* 30, 5087–5100.  
407 <https://doi.org/10.1007/s11269-016-1470-z>.

408 Grimvall, A., Stålnacke, P., 1996. Statistical methods for source apportionment of riverine loads of  
409 pollutants. *Environmetrics* 7(2), 201–213. [https://doi.org/10.1002/\(SICI\)1099-095X\(199603\)7:2<201::AID-ENV205>3.0.CO;2-R](https://doi.org/10.1002/(SICI)1099-095X(199603)7:2<201::AID-ENV205>3.0.CO;2-R).

411 Guo, Y., Wang, X., Melching, C., Nan, Z., 2022. Identification method and application of critical load  
412 contribution areas based on river retention effect. *J. Environ. Manage.* 305, 114314.  
413 <https://doi.org/10.1016/j.jenvman.2021.114314>.

414 Hejzlar, J., Anthony, S., Arheimer, B., Behrendt, H., Bouraoui, F., Grizzetti, B., Groenendijk, P., Jeuken,  
415 M.H.J.L., Johnsson, H., Lo Porto, A., Kronvang, B., Panagopoulos, Y., Siderius, C., Silgram, M.,  
416 Venohr, M., Žaloudík, J., 2009. Nitrogen and phosphorus retention in surface waters: an inter-  
417 comparison of predictions by catchment models of different complexity. *J. Environ. Monit.* 11(3),  
418 584. <https://doi.org/10.1039/b901207a>.

419 Kovacs, A., Honti, M., Zessner, M., Eder, A., Clement, A., Blöschl, G., 2012. Identification of  
420 phosphorus emission hotspots in agricultural catchments. *Sci. Total Environ.* 433, 74–88.  
421 <https://doi.org/10.1016/j.scitotenv.2012.06.024>.

422 Liu, G., Chen, L., Wei, G., Shen, Z., 2019. New framework for optimizing best management practices at  
423 multiple scales. *J. Hydrol.* 578, 124133. <https://doi.org/10.1016/j.jhydrol.2019.124133>.

424 Miller, B.A., Schaetzl, R.J., 2015. Digital classification of hillslope position. *Soil Sci. Soc. Am. J.* 79(1),  
425 132–145. <https://doi.org/10.2136/sssaj2014.07.0287>.

426 Moriasi D. N., Arnold J. G., Van Liew M. W., Bingner R. L., Harmel R. D., Veith T. L., 2007. Model  
427 evaluation guidelines for systematic quantification of accuracy in watershed simulations.  
428 *Transactions of the ASABE.* 50(3), 885–900. <https://doi.org/10.13031/2013.23153>.

429 Nash, J.E., Sutcliffe, J.V., 1970. River flow forecasting through conceptual models part I — A discussion  
430 of principles. *J. Hydrol.* 10(3), 282–290. [https://doi.org/10.1016/0022-1694\(70\)90255-6](https://doi.org/10.1016/0022-1694(70)90255-6).

431 Pionke, H.B., Gburek, W.J., Sharpley, A.N., 2000. Critical source area controls on water quality in an  
432 agricultural watershed located in the Chesapeake Basin. *Ecol. Eng.* 14(4), 325–335.  
433 [https://doi.org/10.1016/S0925-8574\(99\)00059-2](https://doi.org/10.1016/S0925-8574(99)00059-2).

434 Qin, C.-Z., Gao, H.-R., Zhu, L.-J., Zhu, A.-X., Liu, J.-Z., Wu, H., 2018. Spatial optimization of watershed  
435 best management practices based on slope position units. *J. Soil Water Conserv.* 73(5), 504–517.  
436 <https://doi.org/10.2489/jswc.73.5.504>.

437 Rankinen, K., Keinänen, H., Cano Bernal, J.E., 2016. Influence of climate and land use changes on  
438 nutrient fluxes from Finnish rivers to the Baltic Sea. *Agr. Ecosyst. Environ.* 216, 100–115.  
439 <https://doi.org/10.1016/j.agee.2015.09.010>.

440 Rathjens, H., Bieger, K., Chaubey, I., Arnold, J.G., Allen, P.M., Srinivasan, R., Bosch, D.D., Volk, M.,  
441 2016. Delineating floodplain and upland areas for hydrologic models: a comparison of methods.  
442 *Hydrol. Process.* 30(23), 4367–4383. <https://doi.org/10.1002/hyp.10918>.

443 Rathjens, H., Oppelt, N., Bosch, D.D., Arnold, J.G., Volk, M., 2015. Development of a grid-based version  
444 of the SWAT landscape model. *Hydrol. Process.* 29(6), 900–914. <https://doi.org/10.1002/hyp.10197>.

445 Shang, X., Wang, X., Zhang, D., Chen, W., Chen, X., Kong, H., 2012. An improved SWAT-based

446 computational framework for identifying critical source areas for agricultural pollution at the lake  
447 basin scale. *Ecol. Model.* 226, 1–10. <https://doi.org/10.1016/j.ecolmodel.2011.11.030>.

448 Shen, Z., Zhong, Y., Huang, Q., Chen, L., 2015. Identifying non-point source priority management areas  
449 in watersheds with multiple functional zones. *Water Res.* 68, 563–571.  
450 <https://doi.org/10.1016/j.watres.2014.10.034>.

451 Shi, Y.-X., Zhu, L.-J., Qin, C.-Z., Zhu, A.-X., 2021. Spatial optimization of watershed best management  
452 practices based on slope position-field units. *Journal of Geo-Information Science* 23(4), 564–575  
453 (in Chinese with English abstract). <https://doi.org/10.12082/dqxxkx.2021.200335>.

454 Tian, F., Huang, J., Cui, Z., Gao, J., Wang, X., Wang, X., 2020. Integrating multi indices for identifying  
455 priority management areas in lowland to control lake eutrophication: A case study in lake Gehu,  
456 China. *Ecol. Indic.* 112, 106103. <https://doi.org/10.1016/j.ecolind.2020.106103>.

457 Volk, M., Arnold, J.G., Bosch, D.D., Allen, P.M., Green, C.H., 2007. Watershed configuration and  
458 simulation of landscape processes with the SWAT model, in: MODSIM 2007 International Congress  
459 on Modelling and Simulation. Modelling and Simulation Society of Australia and New Zealand,  
460 Christchurch, New Zealand, pp. 2383–2389.

461 Wang, G., Chen, L., Huang, Q., Xiao, Y., Shen, Z., 2016. The influence of watershed subdivision level  
462 on model assessment and identification of non-point source priority management areas. *Ecol. Eng.*  
463 87, 110–119. <https://doi.org/10.1016/j.ecoleng.2015.11.041>.

464 White, M.J., Storm, D.E., Busted, P.R., Stoodley, S.H., Phillips, S.J., 2009. Evaluating nonpoint source  
465 critical source area contributions at the watershed scale. *J. Environ. Qual.* 38(4), 1654–1663.  
466 <https://doi.org/10.2134/jeq2008.0375>.

467 Wolock, D.M., Winter, T.C., McMahon, G., 2004. Delineation and evaluation of hydrologic-landscape

468 regions in the United States using geographic information system tools and multivariate statistical  
469 analyses. *Environ. Manage.* 34, S71–S88. <https://doi.org/10.1007/s00267-003-5077-9>.

470 Yang, D., Herath, S., Musiaka, K., 2002. A hillslope-based hydrological model using catchment area and  
471 width functions. *Hydrolog. Sci. J.* 47(1), 49–65. <https://doi.org/10.1080/02626660209492907>.

472 Zhu, L.-J., Qin, C.-Z., Zhu, A.-X., 2021. Spatial optimization of watershed best management practice  
473 scenarios based on boundary-adaptive configuration units. *Progress in Physical Geography: Earth  
474 and Environment* 45(2), 207–227. <https://doi.org/10.1177/0309133320939002>.

475 Zhu, L.-J., Qin, C.-Z., Zhu, A.-X., Liu, J., Wu, H., 2019. Effects of different spatial configuration  
476 units for the spatial optimization of watershed best management practice scenarios. *Water* 11(2),  
477 262. <https://doi.org/10.3390/w11020262>.

## Figure Captions

**Fig. 1.** Framework of the Markov chain-based PMA identification method using a hierarchy of hydrologically connected spatial units.

**Fig. 2.** Schematization of the spatial discretization scheme and hydrologic connections between spatial units implemented in SWAT<sup>+</sup>. AQU, aquifer; CHA, channel; HRU, hydrologic response unit; LSU, landscape position unit; LAT, lateral flow; PND, pond; RES, reservoir; RHG, groundwater recharge; SUR, surface runoff; TOT, total outflow (specifically, for LSU, it equals to surface runoff plus lateral flow); and numbers represent flow distribution ratio from source unit to receiving unit (adapted from Bieger et al., 2017, 2019, and the source code of SWAT<sup>+</sup> version 59.3).

**Fig. 3.** Construction of flow distribution matrix  $H$  based on upstream-downstream relationships among landscape position units (LSUs) and channels and flow distribution ratios ( $s_1$  and  $s_2$ ) from upland to floodplain.

**Fig. 4.** DEM (a) and landuse map (b) of the Zhongtianshe watershed.

**Fig. 5.** Delineation of three types of spatial units in the SWAT<sup>+</sup> model of Zhongtianshe: (a) subbasin, (b) LSU, (c) HRU (take one subbasin as an example). Each color within the same subbasin in the map of HRU represents one unit, i.e., a particular combination of land use, soil type, and slope classification.

**Fig. 6.** Simulated and observed stream flow during calibration and validation periods.

**Fig. 7.** Simulated and observed total nitrogen (TN) at the calibration period.

**Fig. 8.** Ranking and classification of total nitrogen load contribution at (a) LSU (landscape position unit) level and (b) subbasin level. The labelled number is the ranked sequence of load contribution in descending order. High-contribution areas are identified as PMAs.

**Fig. 9.** Relationships between cumulative areas of spatial units and corresponding load contributions.

Points in (a) present each spatial unit arranged in the descending order of load contribution. Detailed load contribution of landscape position units (LSUs) and subbasins are presented in (b) and (c), respectively.

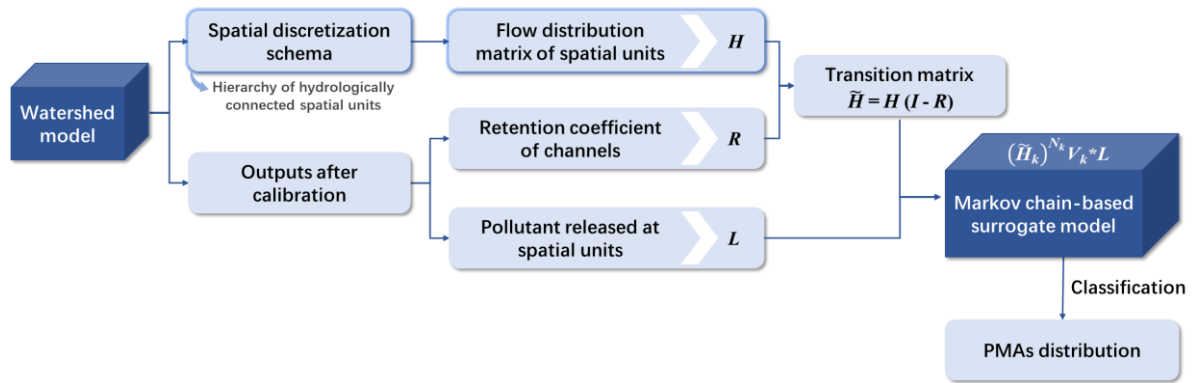


**Fig. 1. Framework of the Markov chain-based PMA identification method using a hierarchy of hydrologically connected spatial units.**

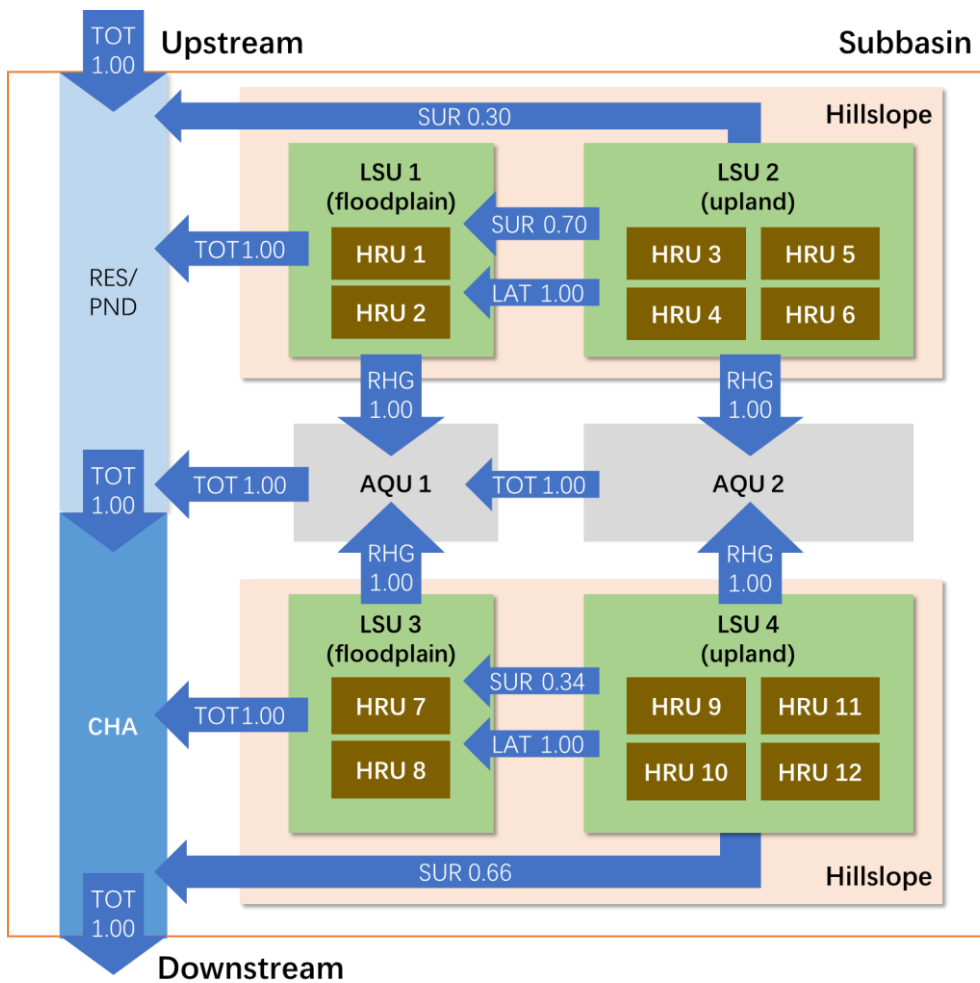
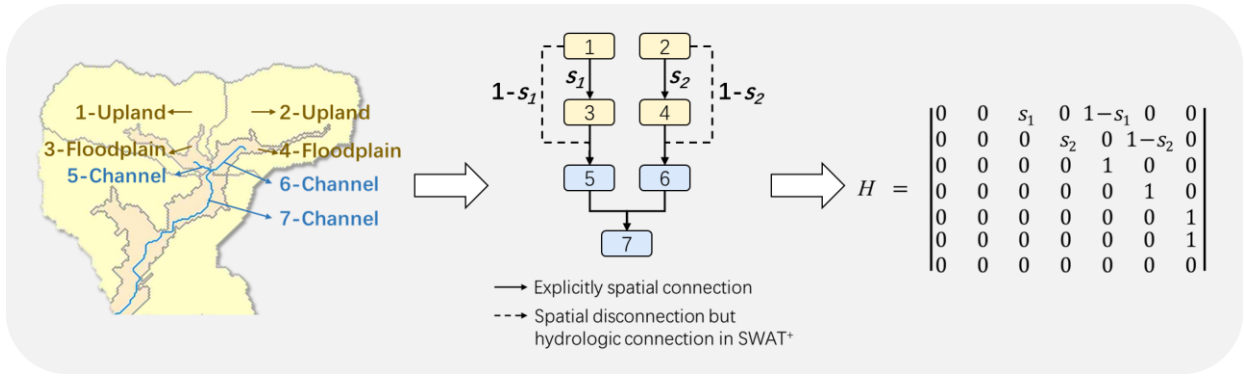
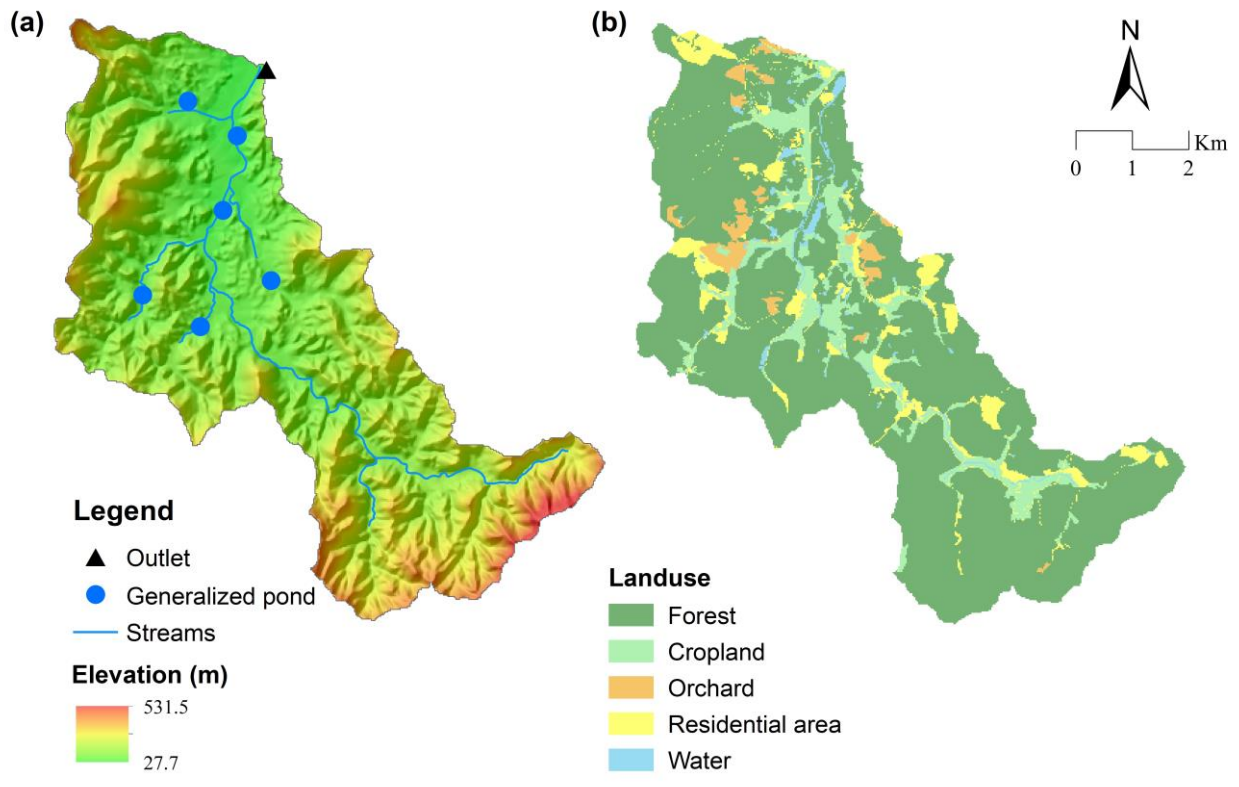


Fig. 2. Schematization of the spatial discretization scheme and hydrologic connections between spatial units implemented in SWAT+. AQU, aquifer; CHA, channel; HRU, hydrologic response unit; LSU, landscape position unit; LAT, lateral flow; PND, pond; RES, reservoir; RHG, groundwater recharge; SUR, surface runoff; TOT, total outflow (specifically, for LSU, it equals to surface runoff plus lateral flow); and numbers represent flow distribution ratio from source unit to receiving unit (adapted from Bieger et al., 2017, 2019, and the source code of SWAT+ version 59.3).



**Fig. 3. Construction of flow distribution matrix  $H$  based on upstream-downstream relationships among landscape position units (LSUs) and channels and flow distribution ratios ( $s_1$  and  $s_2$ ) from upland to floodplain.**



**Fig. 4. DEM (a) and landuse map (b) of the Zhongtianshe watershed.**

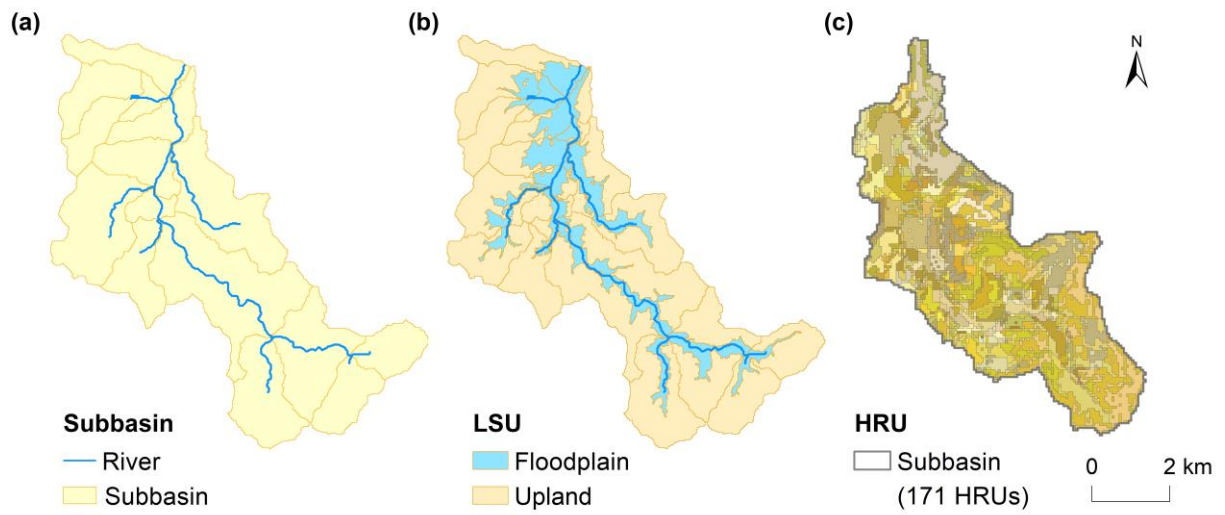


**Fig. 5. Delineation of three types of spatial units in the SWAT<sup>+</sup> model of Zhongtianshe: (a) subbasin, (b) LSU, (c) HRU (take one subbasin as an example). Each color within the same subbasin in the map of HRU represents one unit, i.e., a particular combination of land use, soil type, and slope classification.**

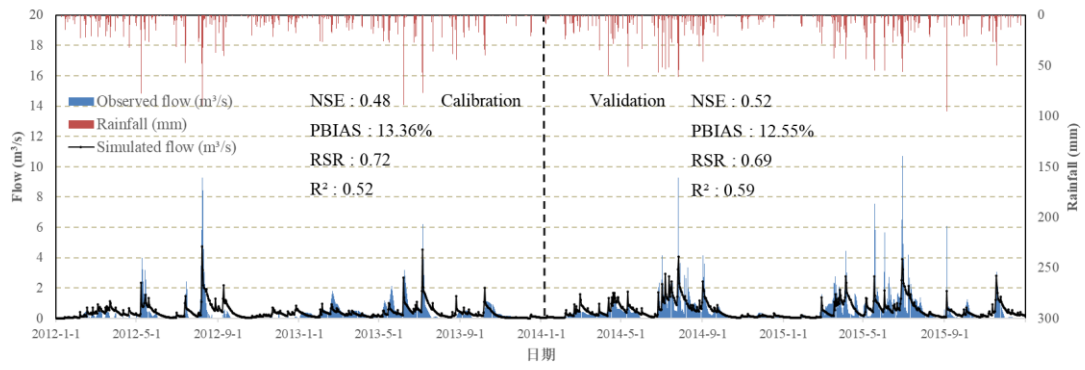


**Fig. 6. Simulated and observed stream flow during calibration and validation periods.**

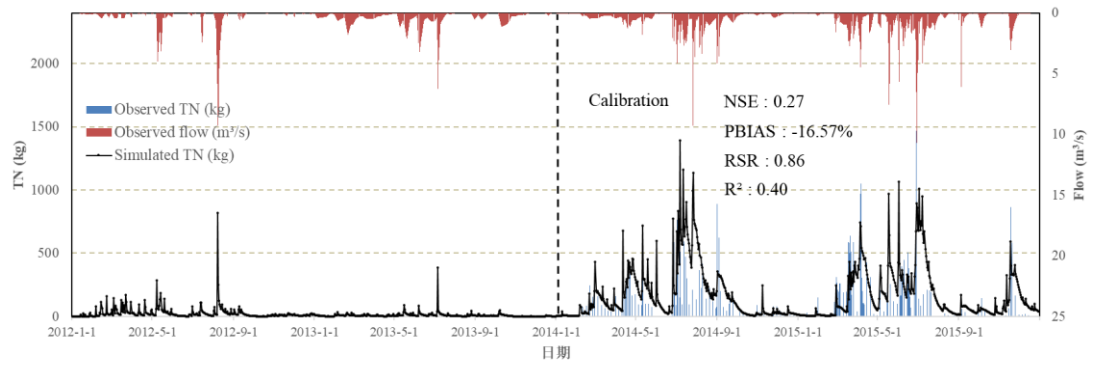


**Fig. 7. Simulated and observed total nitrogen (TN) at the calibration period.**

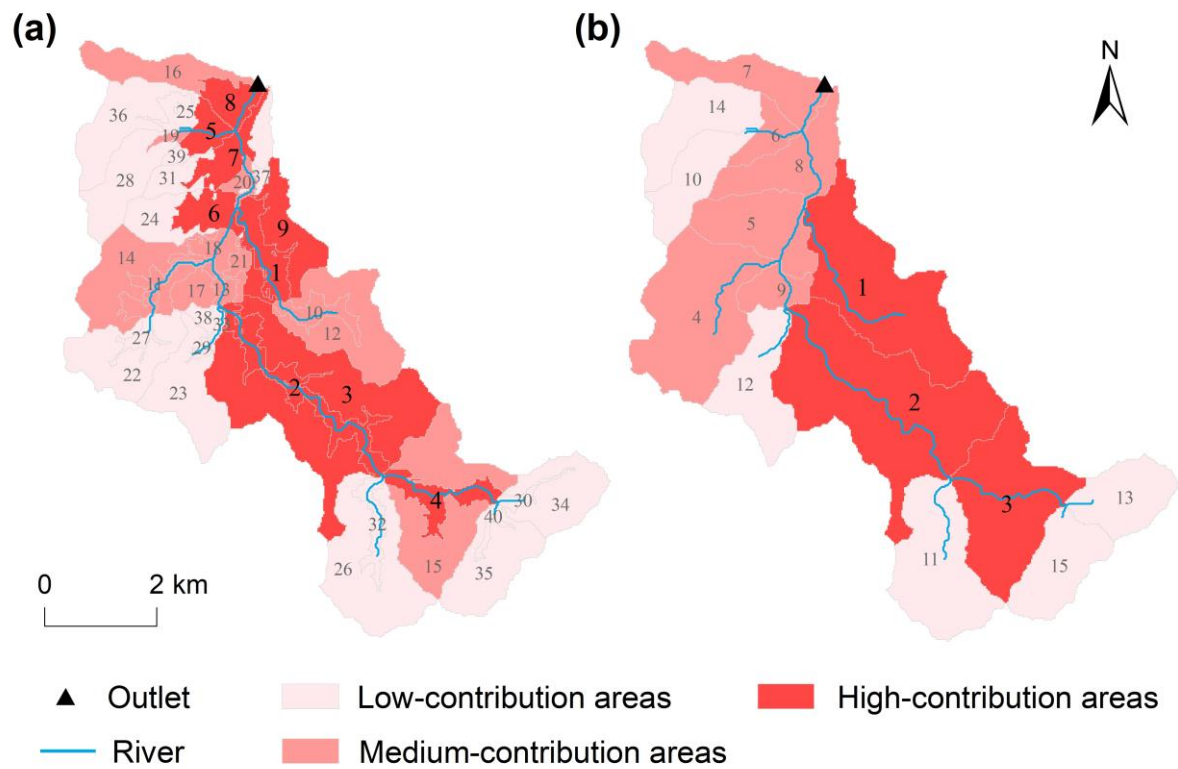


**Fig. 8. Ranking and classification of total nitrogen load contribution at (a) LSU (landscape position unit) level and (b) subbasin level. The labelled number is the ranked sequence of load contribution in descending order. High-contribution areas are identified as PMAs.**

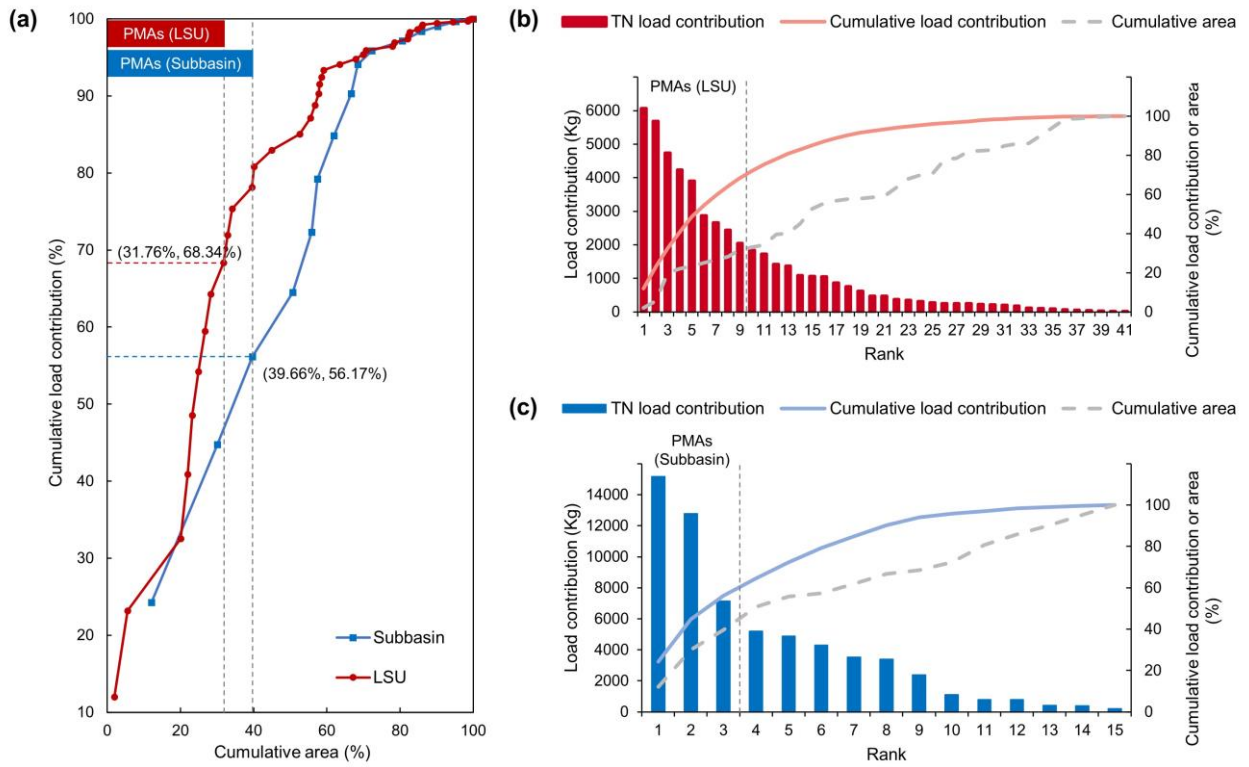


**Fig. 9. Relationships between cumulative areas of spatial units and corresponding load contributions. Points in (a) present each spatial unit arranged in the descending order of load contribution. Detailed load contribution of landscape position units (LSUs) and subbasins are presented in (b) and (c), respectively.**

**Table 1. Data description of the study area.**

Data	Description
DEM	DEM with a resolution of 25 m
Land use	Manually interpreted from Google Earth image derived in 2015
Soil	Soil type map obtained from Soil Science Database of China and soil properties from field sampling
Meteorological data	Daily meteorological data (such as precipitation, temperature, humidity, wind speed and solar radiation) from 2011 to 2015 provided by China Meteorological Data Service Centre and Liyang meteorological station
Agricultural management practices	Cropping and irrigation schedule including crop types and fertilizer usage from field survey
Observed data at the outlet	Daily measured flow (2011–2015) and 5-day measured total nitrogen data (2014–2015) from the site-monitoring station at the watershed outlet

**Table 2. Description of the standard deviation classification method used in this study.**

Load contribution ( $x_i$ )	Level of load pollution
$(-\infty, \bar{x} - 0.5s)$	Low contribution
$(\bar{x} - 0.5s, \bar{x} + 0.5s)$	Medium contribution
$(\bar{x} + 0.5s, +\infty)$	High contribution

$x_i$  denotes the pollutant load contribution of the spatial unit  $i$ ;  $\bar{x}$  and  $s$  denote the mean and the standard deviation of all the units' load contribution, respectively.